Conformation Effects on the Absorption Spectra of Macromolecules

E. Marquez, V. R. Bhethanabotla, and L. H. Garcia-Rubio*

Department of Chemical Engineering, College of Engineering, University of South Florida, Tampa, Florida 33620

Received June 2, 1992; Revised Manuscript Received October 26, 1992

ABSTRACT: Applications of scattering theory to the estimation of absorption coefficients of macromolecules yield values that are different from those obtained from the direct application of the Beer–Lambert law. These differences in absorption coefficients can be explained in terms of the size and optical properties of the macromolecules. This paper reports on the effects of the molecular conformation on the interpretation of the scattering-corrected absorption spectra of macromolecules. Using Monte Carlo simulations, the conformation of polymer chains modeled as self-avoiding walks on a tetrahedral lattice has been investigated. It is demonstrated that the number of chromophores in the trajectory of the incident light varies as a function of the molecular weight. Through an extension of the Beer–Lambert law, the effect of alignment of chromophoric groups is explored and the results are compared with experimentally measured spectra. It is concluded that information on the conformation of macromolecules is contained in the UV–vis spectra and that this information may be quantitatively extracted.

Introduction

The purpose of this paper is to examine the effect of polymer conformation on the absorption spectra of macromolecules in solution. This is achieved, theoretically, through the use of molecular simulations, through the theory of light scattering, and through an extension of the Beer–Lambert law. Conclusions from the theoretical analysis are experimentally supported by careful measurements on commercially available narrow molecular weight distribution polystyrene standards. Motivation for this study stems from the discrepancy found in literature-reported values of the absorption coefficients of macromolecules and on the implications of such differences for the interpretation of the physico-chemical properties of macromolecules in solution.

Absorption spectroscopy studies of homopolymers, copolymers, and proteins have shown significant deviations from the Beer–Lambert law and from the assumption of additivity of the absorption of the individual chromophores.[1-13] Band shifts, solvent effects, and hypochromic effects have been observed as functions of the composition and microstructure of the polymer chains.[2-8] These deviations have been correlated with the sequence length, with tacticity,[3,4,8,10,11] and, in some cases, with the conformation of the molecules in solution.[2,6,9] Deviations from Beer's law have been observed for polymers containing strong chromophores, as well as for polymers containing weakly absorbing groups.[13,14] Recent studies on the information content of spectroscopy data have analyzed the effects of the number of end groups, chemical composition, and polymer microstructure on the absorption spectra.[15,16] In addition, scattering effects due to the molecular size and spectral shifts due to changes in the solvent refractive index have also been reported.[17-19] From these studies, it is apparent that, although it may be possible to interpret the UV–vis spectra in terms of a dominant parameter, in general, no single effect will account for all the deviations reported. For example, Figures 1 and 2 show the scattering-corrected UV–vis spectra of well-characterized narrow polystyrene standards. Notice that, if the scattering corrections were sufficient to explain the observed spectral differences,[17] all the spectra should coincide. Furthermore, if the extinction coefficient at 254 nm is plotted as a function of molecular weight (Figure 3), a well-defined nonlinear behavior becomes apparent. A reasonable explanation of Figures 1–3 is that the spectral differences may be due to the conformation of the polymer in solution.[8,13,14] However, to consider polymer conformation as an important variable in determining the absorption spectra, it is

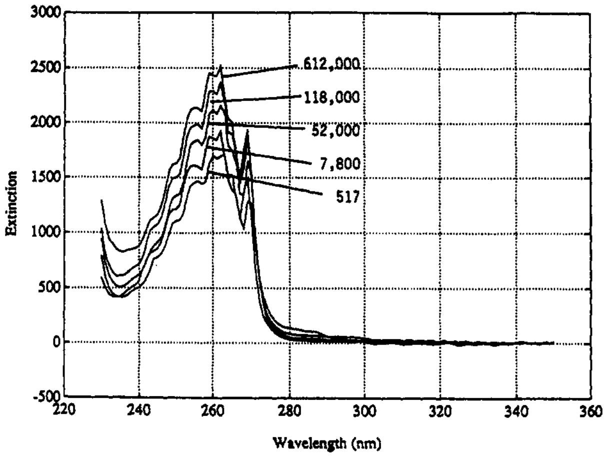

Figure 1. Measured scattering-corrected extinction spectra of narrow polystyrene standards of low and intermediate molecular weights in THF at 25 °C. The molecular weights are indicated.

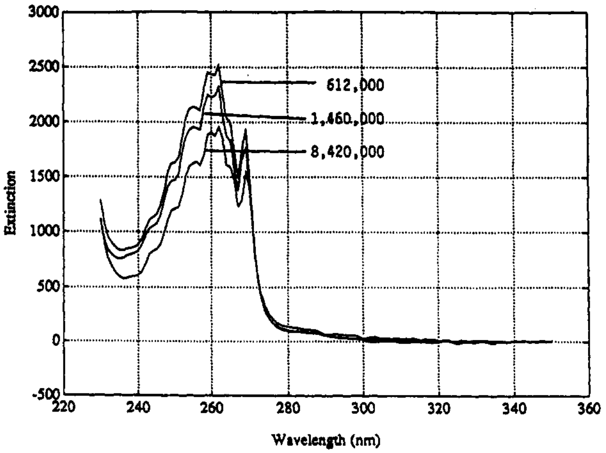

Figure 2. Measured scattering-corrected extinction spectra of narrow polystyrene standards of high molecular weights in THF at 25 °C. The molecular weights are indicated. Note the reversal in the trend compared to Figure 1.

0024-9297/93/2226-0479$04.00/0

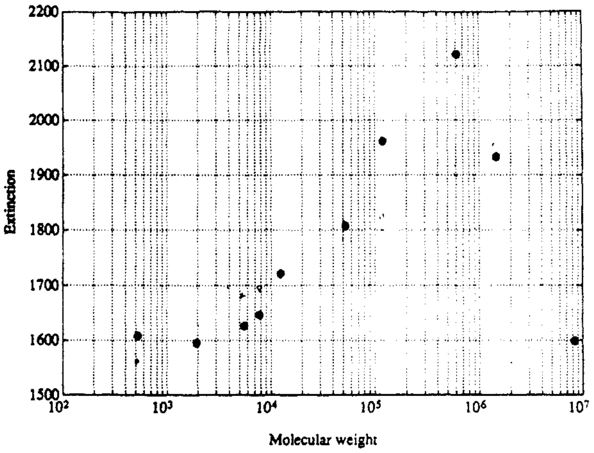

Figure 3. Nonlinear behavior of the measured absorption coefficient of polystyrene standards in THF at λ = 254 nm.

Table I

M_w	M_n	ϵ_0 (254 nm)	$\langle R_g \rangle^a$	$n_n \times 10^{-6\ b}$
517	503	1607.75	16.67	8.575
1 940	1 690	1594.54	32.42	8.644
5 480	5 200	1625.82	53.97	8.478
7 820	7 400	1646.41	64.06	8.372
12 200	12 000	1721.04	78.26	8.009
52 100	50 400	1806.99	157.83	7.628
118 000	107 000	1961.27	228.00	7.029
612 000	556 000	2121.76	499.22	6.496
1 460 000	1 200 000	1932.51	807.99	7.137
8 420 000	7 196 580	1598.18	2133.56	9.079

[a] $\langle R_g \rangle$ (in Å) calculated from eq 4 or eq 11. [b] n_n (in number/cm^3) assuming a constant $M/\langle R_g \rangle^2$.

necessary to demonstrate that indeed optical effects are possible as a result of the polymer conformation and, then, to quantitatively incorporate these effects into the interpretation model. For this purpose, the analysis has been divided into three sections; the first section deals with possible optical effects due to polymer conformation in the context of Mie theory and the Beer–Lambert law; in the second section it is demonstrated, using molecular simulation techniques, that alignment of chromophoric groups is likely to occur; the third section deals with the comparison between model predictions and experimentally determined absorption spectra of narrow molecular weight distribution polystyrene standards. Before presenting the analysis, a brief description of the experimental work is given.

Experimental Methods

Narrow polystyrene standards (Scientific Polymer Products, Inc.) were dissolved in spectral-grade tetrahydrofuran (Burdick and Jackson Laboratories) at several carefully predetermined concentrations. The UV–vis spectra were recorded on a Perkin-Elmer 3840 photodiode array UV–vis spectrophotometer equipped with a thermoelectric cell holder and a temperature controller with temperature-programming capabilities. A 1-cm-path-length cell was used for all measurements. The turbidity spectra of the polystyrenes were obtained from measurements at several concentrations. Up to seven concentrations plus replicates were used to obtain good estimates of the optical constants as well as good estimates of the measurement errors. Special care was taken to ensure that the measurements were always within the linear range of the instrument. The spectroscopy data were stored in a Perkin-Elmer 7500 computer and analyzed using the interpretation software developed in house. The scattering-corrected spectra are shown in Figures 1 and 2, and the measured extinction at 254 nm is reported in Table I.

Optical Effects and Molecular Conformation

In standard UV–vis transmission spectroscopy measurements using unpolarized light, conformation effects may become evident through changes in the absorption and scattering components of the spectra. If a random coil is hypothesized as shown in Figure 4 and a beam of light is considered to traverse the molecule, the number of chromophoric groups in the trajectory of the light (i.e., the segment density) will determine the amount of light that will be scattered or absorbed.[20] Furthermore, if it is assumed that the cross section of a molecule can be approximated by the cross section defined by the effective scattering volume, the dimensions of the cross section, when estimated from experimental data, will reflect scattering effects due to the alignment of functional groups within the molecule. In addition, it is known that, for small absorbing particles in the Rayleigh regime, the scattering component will be small relative to the absorption component of the spectra.[20,21] Therefore, for macromolecules, chromophore alignments and density changes resulting from molecular conformations are expected to be reflected primarily through changes in the absorption coefficient.

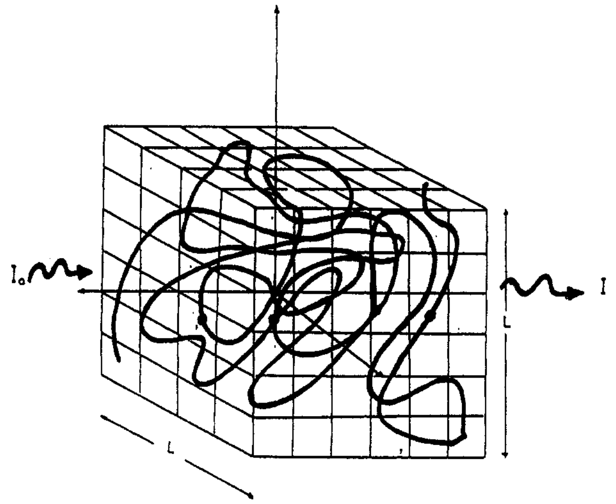

Figure 4. Ideal random coil contained in a cube of dimensions equal to the end-to-end distance of the chain. I_0 represents the incident radiation, and the full circles represent the chromophores aligned in the direction of I_0.

To analyze the effect of polymer conformation on the absorption coefficient, consider a polymer molecule with chain length N enclosed in a cube of dimensions equal to the end-to-end distance (L) of the molecule (Figure 4), where the area (A) facing the incident radiation is divided into Z subareas equal to the absorption cross-sectional area of a single chromophore (α).

$$Z = L^2 = A/\alpha \tag{1}$$

In addition, assume that there will be only one chromophore in every occupied cell in the lattice and that the Beer–Lambert law is applicable to every volume element in the cube. For an incoming beam of intensity I_0 and wavelength λ, it can be readily shown that the transmission across the cube is given by

$$(I/I_0)_\lambda = (1/Z)\sum_i^L \sum_j^L \exp[-\epsilon'(\lambda)\, M_0 n(i,j)/(N_{av}\alpha)] \tag{2}$$

where $\epsilon'(\lambda)$ represents the absorption coefficient per chromophore (cm^2/g), M_0 is the molecular weight of the chromophoric groups, N_{av} is Avogadro's number, and $n(i,j)$ represents the number of chromophores contained in the volume element defined by the subarea with coordinates (i, j). Notice that $n(i,j)$ also represents the number of chromophoric groups aligned in the direction of the incident beam.

Replacing Z from eq 1 into eq 2 and expanding the exponential term, an expression in terms of the moments of the distribution of alignments per unit area is obtained:

$$(I/I_0)_\lambda = 1 - \epsilon(\lambda)\mu_0 + \epsilon(\lambda)^2\mu_1/2! - \epsilon(\lambda)^3\mu_2/3! + \ldots \quad (3)$$

where μ_n represents the nth moment of the distribution of alignments.

Alternatively, eq 3 can be expressed in terms of the averages of the distribution of alignments

$$(I/I_0)_\lambda = 1 - \epsilon' N[1 - \epsilon'(n_n/2)(1 - \epsilon'(n_w/3)(1 - \ldots))] \quad (4)$$

$$\epsilon' = \epsilon(\lambda)\, M_0/N_{av}L^2 \quad (5)$$

where n_n and n_w represent the number- and weight-average number of alignments.

Equations 4 and 5 describe the dependence of the overall absorption coefficient

$$\epsilon_0(\lambda) = \ln\,(I_0/I) \quad (6)$$

on the molecular dimensions and on the distribution of chromophore alignments. Notice that eq 2 can be used to approximate any geometry. If a different geometry is used, L represents a characteristic dimension and ϵ' will contain the corresponding form factor.

Although eqs 4 and 5 provide a conceptual basis for the understanding of conformation effects on the overall Beer–Lambert absorption coefficient, use of eq 4 is difficult because the form of the distribution of alignments is unknown (see next section). Nevertheless, similar insights may be obtained if it is realized that the probability of alignments for the chromophoric groups should be related to the distribution of chain segments relative to the center of mass (i.e., the segment density).

The approximate distribution of segments, for a Gaussian chain, as a function of the distance from the center of mass (r) and of the radius of gyration ($\langle R_g\rangle$) is given by[22-24]

$$\rho(r) = (M/N_{av})(3/2\pi\langle R_g\rangle^2)^{3/2}\exp(-3r^2/2\langle R_g\rangle^2) \quad (7)$$

where $\rho(r)$ is the segment density in grams per cubic centimeter and M represents the polymer molecular weight.

If the area facing the incoming radiation (I_0) is now considered to be the circle defined by the radius of gyration, the density projected onto the surface is given by

$$\tilde{\rho}(r) = (M/N_{av})(3/2\pi\langle R_g\rangle^2)^{3/2}\sum_{m=1}^{\infty}(-3/2(1 - r^2/\langle R_g\rangle^2))^m/ (2m + 1)m! \quad (8)$$

and the transmission across the sphere will be given by

$$(I/I_0)_\lambda = (2/\langle R_g\rangle)\int_0^{R_g}\exp(-2\epsilon(\lambda)\,\bar{\rho}(r)\,\langle R_g\rangle)\,r\,\mathrm{d}r \quad (9)$$

Expanding the exponential in the power series and keeping only the leading term, eq 9 can be readily integrated to yield

$$(I/I_0)_\lambda = 1 - \beta\sum_{m=1}^{\infty}(-3/2)^m/[(m + 1)!(2m + 1)] \quad (10)$$

$$\beta = \epsilon(2M/N_{av}\langle R_g\rangle^2)(3/2\pi)^{3/2}$$

Since $\beta \ll 1$ for absorption coefficients typical of macromolecules, to a good approximation, eq 10 can be simplified to

$$(I/I_0)_\lambda = \exp(-\kappa\epsilon(\lambda)\,M/\langle R_g\rangle^2) \quad (11)$$

$$\kappa = (2/N_{av})(3/2\pi)^{3/2}\sum_{m=1}^{\infty}(-3/2)^m/[(m + 1)!(2m + 1)]$$

Equation 11 indicates that, to a first approximation, the overall Beer–Lambert absorption coefficient ($\epsilon_0(\lambda)$) is directly proportional to the molecular weight of the polymer and inversely proportional to the square of its radius of gyration. This is in agreement with the first term in eq 4. It is clear that the combined effects of the radius of gyration and molecular weight play an important role in explaining the behavior shown in Figures 1–3. The expected variations of the extinction coefficient as functions of molecular weight and radius of gyration for values typical of macromolecules[25-27] are shown in Figures 5 and 6.

Equations 4 and 11 enable the use of Mie theory for the joint estimation of the radius of gyration and the molecular weight directly from turbidity measurements. To use Mie theory for the interpretation of the turbidity spectra of macromolecules, it is necessary to calculate the Mie absorption coefficient in terms of the Beer–Lambert absorption coefficient through Bouger's law[17,20]

$$k(\lambda) = \lambda\epsilon_0(\lambda)/4\pi \quad (12)$$

The complete interpretation model is now given by either eq 4 or eq 11, by eq 12, and by Mie scattering formulas.[20] However, it remains to be demonstrated that the alignment of chromophoric groups is likely to occur for macromolecules in solution and to obtain estimates on the probability of alignments as a function of the molecular weight to assess the order of magnitude of the expected conformation effects. Both of these objectives are explored using Monte Carlo simulation of ideal polymer chains.

Likelihood of Chromophore Alignments

A simple model of a single homopolymer chain in a good solvent was utilized to study the probabilities of alignment and segment density distributions. Self-avoiding walks (SAWs) were simulated on a tetrahedral lattice using known Monte Carlo methods.[28] To generate sizable samples of large chains, the chain-enrichment algorithm, originally conceived by Wall and Erpenbeck,[29] was implemented. In this method, two integers s and p are chosen such that they satisfy

$$\exp(\zeta s) = p + \delta \quad (13)$$

where δ is a small positive number and ζ is the attrition constant. The parameter ζ depends only on the type of walk and lattice (0.041 for SAWs on a three-dimensional tetrahedral lattice). The attrition constant relates the number of walks reaching size n (N_n) to the number of walks attempted (N_0) through

$$N_n = N_0\exp(-\zeta n) \quad (14)$$

In the simulation, every segment of the walk that reaches s steps is continued p times. By choosing s and p that satisfy eq 14, umbiased samples of longer chains with a fair variety of chain beginnings can be generated. We have chosen three sets of s and p [(18, 2), (28, 3), and (39, 4)] to produce sizable numbers of chains up to 1000 steps long. Double-linked lists were used in the program implementation to increase search efficiency. The mean-square radius of gyration and mean-square end-to-end distance were calculated for the first few runs (of 1 million trials each) to check the computer program. Prefactors

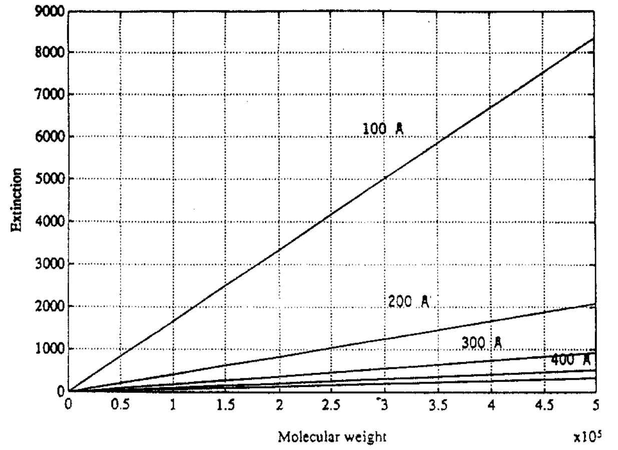

Figure 5. Dependence of the overall Beer–Lambert absorption coefficient on the molecular weight for the indicated values of the radius of gyration.

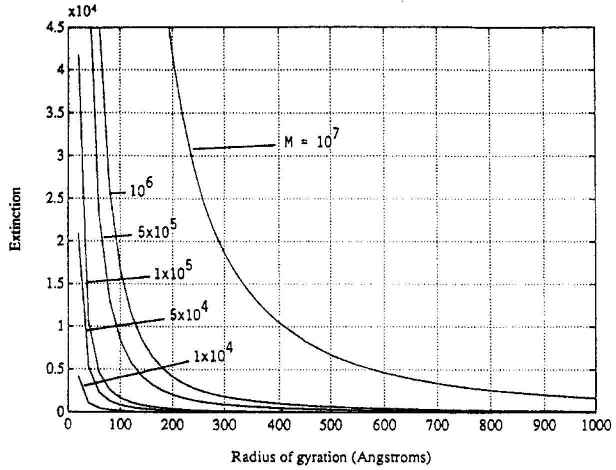

Figure 6. Dependence of the overall Beer–Lambert absorption coefficient on the radius of gyration for the indicated molecular weights.

and exponents in the scaling relations of these quantities agree excellently with literature values.[29,30]

Probabilities of alignments as functions of the chain length were calculated as averages over simulated configurations. These were defined as

$$p_i(N) = \langle a_i(N)/\sum_i a_i(N)\rangle \qquad (15)$$

where $p_i(N)$ is the probability of i nodes (mers) being aligned for a chain length N, a_i is the number of alignments of i nodes for a given configuration of the chain, and the brackets denote averaging over simulated configurations. Alignments in the three directions parallel to the Cartesian axis were averaged to improve statistics.

Results for alignments up to 5 nodes as functions of chain length are shown in Figures 7 and 8. The probability of finding an unaligned node decreases rapidly to about 0.94 and appears not to change much with chain length, at least up to the 1000 node chains simulated. Of the alignments present, 2 nodes are the most probable ($p_i \sim 0.05$ for large N), with higher node alignments being much less likely. The number of 6 and higher node alignments were found to be negligible in a typical run of 1 million trials. The single-node alignment probability appears to turn around and increase for larger chain lengths with a consequent decrease in higher node alignments. Clearly, the overall segment density decreases as the chain length becomes larger. Whether this leads to a decrease in higher node alignments is difficult to guess. Simulations of much larger chains should clarify this point further. However, precise calculation of alignment probabilities is computationaly expensive for two reasons. First, a very large number of configurations is possible for larger chains, and a substantial sample of these is necessary to calculate alignments precisely. In fact, 100 runs of a million trials

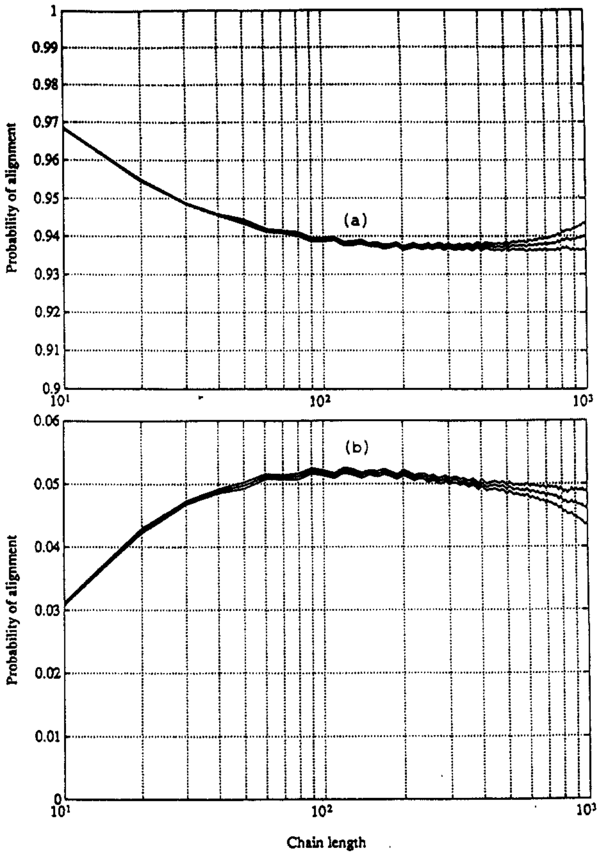

Figure 7. Probability of alignments of 1 (a) and 2 (b) nodes as functions of the number of segments for SAWs on a tetrahedral lattice. The 95% confidence intervals are indicated.

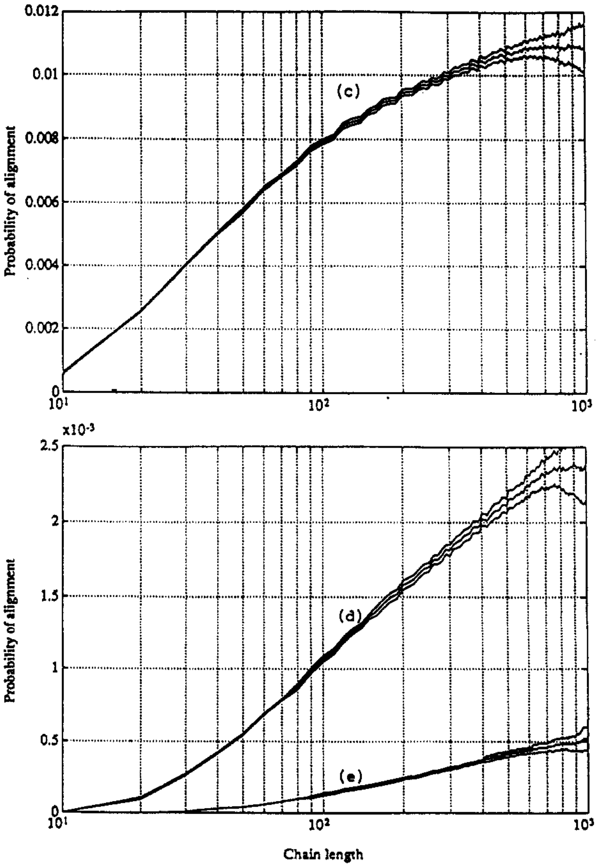

Figure 8. Same as Figure 7 but for 3 (c), 4 (d), and 5 (e) node alignments.

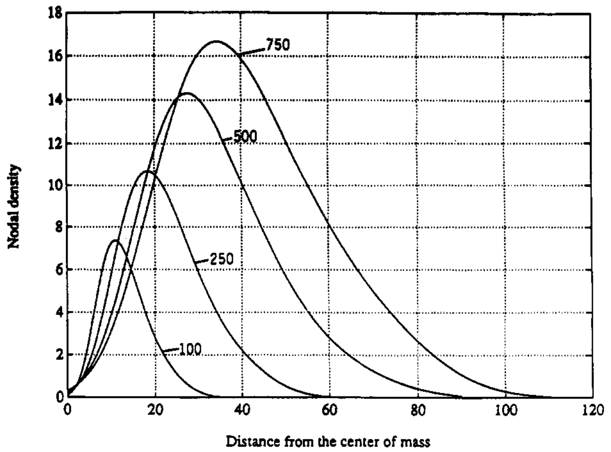

Figure 9. Three-dimensional segment densities as functions of the distance from the center of mass for several chain lengths. The values for the chain lengths are indicated.

each were necessary to produce the statistical precision reported in Figures 7 and 8 (the 95% confidence intervals are shown with each run considered an independent sample). Second, despite the enrichment procedure adapted, only a small fraction of the trials reach long chain lengths. This of course depends on the choice of s and p, but the alternative pivot algorithm may prove much more efficient for simulating longer chains, especially if only a few specific chain lengths are desired.[30]

In the previous section, an approximation to the segment density projected onto the plane perpendicular to the incident radiation was used as a related measure to develop an interpretation model for the data. These densities are easily obtained from simulation. In fact, they are unambiguously defined for off-lattice models of the polymer chains, which is not the case with alignment probabilities. Use of the segment density as a measure is also appealing because much shorter runs are necessary to estimate them precisely.

Simulated three-dimensional segment densities as functions of the distance from the center of mass for chains of length 100, 250, 500, and 750 are shown in Figure 9. Distributions of segments as functions of the radial distance were calculated first and then numerically differentiated to obtain the densities. Thus, integrals of these functions give the total number of nodes directly. These functions are fitted well to an exponential of a fourth-order polynomial for all chain lengths. (The fit is worse at very small chain lengths, and, hence, the curves in Figure 9 do not go through the origin.) They differ from the Gaussian function assumed in the previous section, which in fact is the distribution of end-to-end distances for self-intersecting walks.[31] Projected densities are expected to have shapes similar to the three-dimensional ones. Effects of solvent conditions, temperature, and chain composition (i.e., models for copolymers) can be incorporated into these lattice models quite easily by introducing interaction potentials among chain segments. These effects will change both the alignment probabilities and the segment density distributions. Such calculations are now underway.

It can be concluded from these simulations that segment density distributions are better defined and easier to estimate than alignment probabilities. Either are measures of the chain internal structure (conformation), and, although establishment of a direct correspondence is difficult, it is clear that interpretation models for spectroscopy data can be constructed using either measures and lead to similar conclusions (i.e., eqs 4 and 11).

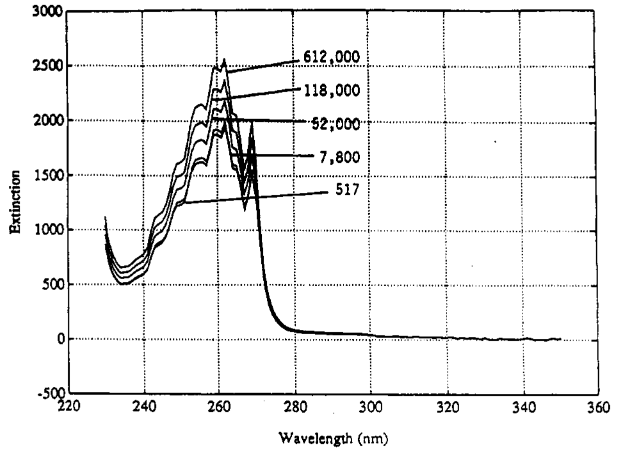

Figure 10. Predicted effects of the molecular conformation on the absorption spectra of low and intermediate molecular weight polystyrene standards. The spectrum of a narrow molecular weight distribution polymer (M_w = 118 000) was used as a basis for the calculations.

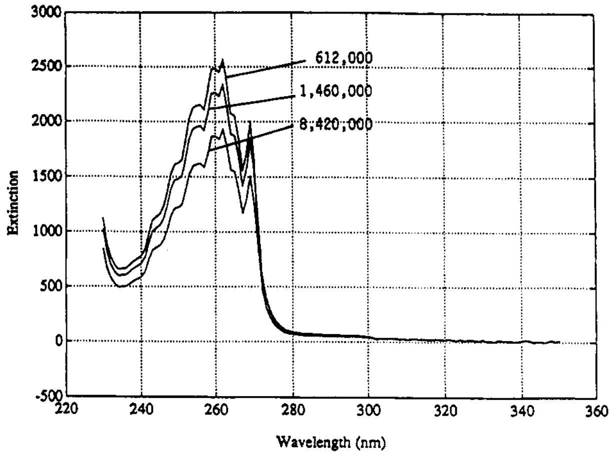

Figure 11. Predicted effects of the molecular conformation on the absorption spectra of high molecular weight polystyrene standards. The spectrum of a narrow molecular weight distribution polymer (M_w = 118 000) was used as a basis for the calculations.

Comparison of Model Predictions with Experimental Data

Deviations from the Beer–Lambert law observed for the scattering-corrected absorption spectra of narrow molecular weight distribution polystyrene standards are evident in Figures 1 and 2. To establish if the molecular conformation effects predicted by eqs 4 and 11 can explain the experimental observations, changes in the ratio $M/\langle R_g\rangle^2$ have been superimposed on the experimentally measured spectrum of a 118 000 molecular weight standard. Values for the ratio $M/\langle R_g\rangle^2$ were calculated by first estimating the radius of gyration for the 118 000 standard from values reported for toluene as the solvent.[26] This was considered an adequate approximation because the Mark–Houwink parameters for polystyrene in toluene and in THF are reasonably close.[26,27] From the spectrum of the 118 000 molecular weight standard and the calculated radius of gyration, an estimate of the absorption coefficient per chromophore can be obtained from either eq 4 or eq 11. The radius of gyration for each standard was then calculated from the measured absorption coefficients at 254 nm (Table I). The spectra shown in Figures 10 and 11 were calculated from the known molecular weights, the calculated radius of gyration, and the estimated absorption coefficient per chromophore. By comparing Figures 1 and 2 with Figures 10 and 11, it is evident that the absorption behavior of macromolecules can be accounted for through either eq 4 or eq 11. Furthermore,

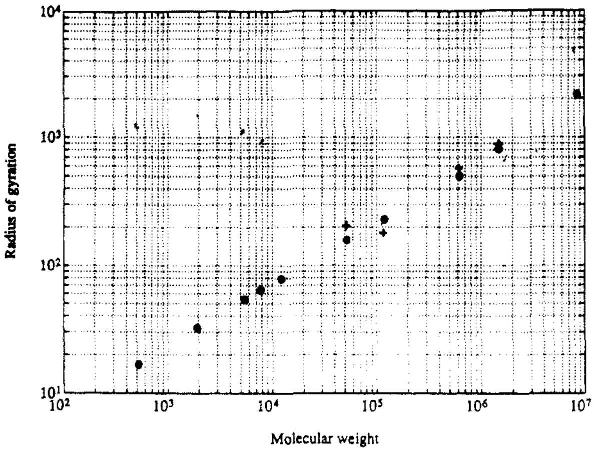

Figure 12. Radius of gyration calculated from the measured extinction at 254 nm using as reference a narrow standard with M_w = 118 000: (O) calculated values; (+) values reported by the manufacturer.

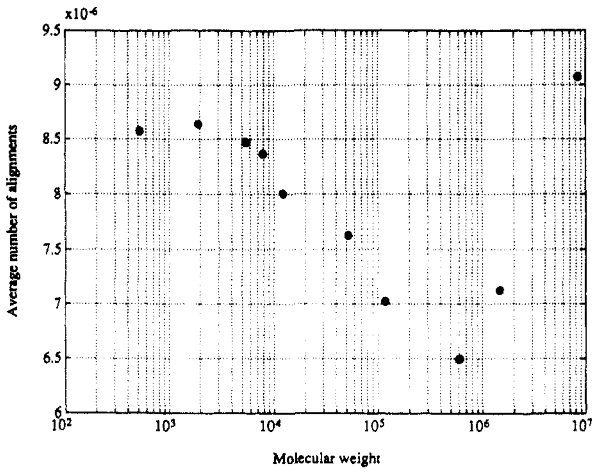

Figure 13. Number-average number of alignments calculated from measured extinction values at 254 nm, using as reference a narrow standard with M_w = 118 000.

the calculated radii of gyration show a monotonic increase as a function of the molecular weight (Figure 12), and there is fair agreement between the calculated radii of gyration and the values reported by the manufacturer.

It is clear that changes in the ratio $M/\langle R_g\rangle^2$, which reflect changes in the molecular density, can explain the observed spectroscopy behavior. Furthermore, existing literature data suggest that the mean-square radius of gyration is proportional to $N^{6/5}$ where N is the number of segments (mers) in the chain,[25,26,32] thus implying that the ratio $M/\langle R_g\rangle^2$ is a weak function of M (i.e., $M^{-1/5}$). Therefore, if this weak dependence is neglected and it is assumed that $M/\langle R_g\rangle^2$ is constant, then to explain Figures 1 and 2, it is necessary to consider at least one additional term in eq 4 (i.e., n_n). Figure 13 shows the number-average number of alignments calculated under the assumption of a constant $M/\langle R_g\rangle^2$. Notice that the values obtained are in agreement with expected segment densities for macromolecules.[22]

As can be appreciated from Figures 10–13, the results suggest that the modified Beer–Lambert law (eqs 4 and 11) can be used in conjunction with Mie theory, to interpret the UV–vis spectra of macromolecules in solution. However, to apply the complete interpretation model, it is necessary to have reliable estimates of the absorption coefficient per chromophoric unit. Such estimates can be readily obtained through the analysis of a complete series of narrow standards. Quantitative analysis of a series of polystyrene standards and the details of the estimation procedure will be reported separately.

Summary and Conclusions

Effects of molecular conformation on the interpretation of the scattering-corrected absorption spectra of macromolecules have been investigated by considering possible alignments of chromophoric groups within the scattering volume of the macromolecules. Two equivalent models that relate measurable fundamental polymer properties such as molecular weight, radius of gyration, and segment density have been derived to quantify possible conformation effects. These models are applicable within the context of Mie scattering theory. Using Monte Carlo simulations, the conformation of a simple model of a polymer chain in a good solvent has been investigated and it has been demonstrated that chromophore alignments are likely to occur and that the number of chromophores in the trajectory of the incident light varies as a function of the molecular weight. Comparison of experimentally measured spectra with the effects calculated through the proposed extension of the Beer–Lambert law leads to the conclusion that information on the conformation of macromolecules is contained in the UV–vis spectra and that this information may be quantitatively extracted.

Acknowledgment. This research was supported by the NSF Initiation Grant RII-8507956 and by a Grant from Indesca, Venezuela. Computer time was provided by the University of South Florida Computing Services. The authors are indebted to J. Mittman and F. Quinlan for careful measurement of the extinction coefficients and to Dr. J. C. Busot for many useful discussions.

References and Notes

(1) Meehan, E. J. *J. Polym. Sci.* **1945**, *1* (3), 175.
(2) Vala, M. T.; Rice, S. A. *J. Chem. Phys.* **1963**, *39*, 2348.
(3) O'Driscoll, K. F.; Wertz, W.; Husar, A. J. *J. Polym. Sci.* **1967**, *5*, 2159.
(4) Brussau, R. J.; Stein, D. J. *Angew. Makromol. Chem.* **1970**, *12*, 59.
(5) Acosta, J. L.; Sastre, R. *Rev. Plast. Mod.* **1973**, *24* (205), 67.
(6) Gallo, B. M.; Russo, S. *J. Macromol. Sci., Chem.* **1974**, *33*, 521.
(7) Gallo, B. M.; Russo, S. *Adv. Chem. Ser.* **1974**, *142*, 85.
(8) Stutzel, B.; Miyamoto, T.; Cantow, H. *Polym. J.* **1976**, *8* (3), 1976.
(9) Noel, C.; Monnerie, L. *Polym. J.* **1976**, *8* (4), 319.
(10) Gruber, E.; Knell, W. L. *Makromol. Chem.* **1978**, *179*, 733.
(11) Garcia-Rubio, L. H.; Hamielec, A. E.; MacGregor, J. F. *ACS Symp. Ser.* **1982**, *197*, 151.
(12) Garcia-Rubio, L. H. *J. Appl. Polym. Sci.* **1982**, *27*, 2043.
(13) Kang-Jen, L.; Linowski, J. S.; Ullman, R. *Makromol. Chem.* **1967**, *105*, 18.
(14) Ohara, K. *Polym. J.* **1971**, *2*, 109.
(15) Garcia-Rubio, L. H.; Ro, N.; Patel, R. D. *Macromolecules* **1984**, *17*, 1998.
(16) Garcia-Rubio, L. H.; Ro, N. *Can. J. Chem.* **1985**, *63*, 253.
(17) Garcia-Rubio, L. H. *Macromolecules* **1987**, *20*, 3070.
(18) Garcia-Rubio, L. H. *Macromolecules*, in press.
(19) Duysens, L. N. M. *Biochim. Biophys. Acta* **1956**, *19*, 1.
(20) van de Hulst, H. C. *Light Scattering by Small Particles*; Wiley: New York, 1957.
(21) Penndorf, R. B. *J. Opt. Soc. Am.* **1962**, *52*, 896.
(22) Debye, P.; Bueche, F. *J. Chem. Phys.* **1952**, *20*, 1337.
(23) Flory, P. J. *Principles of Polymer Chemistry*; Cornell University Press: Ithaca, NY, 1953.
(24) Kumar, A.; Gupta, S. K. *Fundamentals of Polymer Science and Engineering*; Tata McGraw-Hill: New Delhi, 1978.
(25) Outer, P.; Carr, C. I.; Zimm, B. H. *J. Chem. Phys.* **1950**, *18*, 830.
(26) Brandrup, J.; Immergut, E. H. *Polymer Handbook*; Wiley-Interscience: New York, 1975.
(27) Yau, W.; Bly, D. *Modern Size Exclusion Chromatography*; Wiley-Interscience: New York, 1979.
(28) Kremer, K.; Binder, K. *Comput. Phys. Rep.* **1988**, *7*, 259.
(29) Wall, F. T.; Erpenbeck, J. J. *J. Chem. Phys.* **1959**, *30*, 634.
(30) Zifferer, G. *Macromolecules* **1990**, *23*, 3166.
(31) Edwards, S. F. *Proc. R. Soc. London* **1965**, *85*, 613.
(32) de Gennes, P.-G. *Scaling Concepts in Polymer Physics*; Cornell University Press: Ithaca, NY, 1979.